A seasonal analysis of aerosol NO_3^- sources and NO_x oxidation pathways in the Southern Ocean marine boundary layer

Jessica M. Burger[1], Emily Joyce[2], Meredith G. Hastings[2], Kurt A. M. Spence[1], Katye E. Altieri[1]

[1]Department of Oceanography, University of Cape Town, Rondebosch, 7701, South Africa
[2]Department of Earth, Environmental and Planetary Sciences and Institute at Brown for Environment and Society, Brown University, Providence, RI, 02906, USA.

Correspondence to: Jessica M. Burger (brgjes006@uct.ac.za)

Supplemental material

Table S1. The start and end date of each filter deployment, as well as the latitude (º N) and Longitude (º E) at the start and end of each filter deployment are presented. The duration (hr) of each filter deployment and the number of daylight hours experienced during each filter deployment is also included, and samples are separated by season (Winter, Spring and Summer) and by transect (Southbound, Northbound or Ice edge).

Season	Sample	Transect	Start date	End date	Latitude (º N)		Longitude (º E)		Duration (hr)	Daylight (hr)
			(yyyy/mm/dd)	(yyyy/mm/dd)	Start	End	Start	End		
Winter	1	Southbound	2019/07/19	2019/07/20	-35.6	-39.0	16.4	12.9	24.5	9.9
Winter	2	Southbound	2019/07/20	2019/07/22	-39.4	-46.3	12.5	6.2	30.2	9.5
Winter	3	Southbound	2019/07/23	2019/07/24	-50.9	-54.5	2.6	-0.3	20.3	8.4
Winter	4	Northbound	2019/07/28	2019/07/30	-56.4	-52.7	0.6	-1.7	29.8	8.4
Winter	5	Northbound	2019/08/02	2019/08/03	-45.0	-42.5	6.6	8.9	19.5	9.8
Winter	6	Northbound	2019/08/03	2019/08/05	-42.3	-36.3	9.1	13.3	21.9	10.2
Spring	1	Southbound	2019/10/13	2019/10/14	-35.8	-38.8	14.9	11.7	24.4	13.0
Spring	2	Southbound	2019/10/14	2019/10/16	-40.3	-44.7	10.6	6.9	25.6	13.2
Spring	3	Southbound	2019/10/16	2019/10/17	-44.9	-48.4	6.7	4.2	23.7	13.5
Spring	4	Southbound	2019/10/17	2019/10/19	-48.4	-54.0	4.2	0.0	29.9	13.8
Spring	5	Southbound	2019/10/19	2019/10/20	-54.0	-55.0	0.0	0.2	17.1	14.1
Spring	6	Southbound	2019/10/20	2019/10/21	-55.0	-55.2	0.2	0.2	11.9	14.3
Spring	7	Southbound/ Ice edge	2019/10/21	2019/10/23	-55.2		0.2		29.5	14.3
Spring	8	Ice edge	2019/10/23	2019/10/24		-59.3		0.0	20.3	15.0
Spring	9	Ice edge	2019/10/24	2019/10/26	-59.3	-59.1	0.0	1.0	17.7	15.0
Spring	10	Ice edge	2019/10/26	2019/10/28	-58.9	-59.3	1.2	6.6	17.5	15.2
Spring	11	Ice edge	2019/10/28	2019/10/30	-59.3	-59.3	6.6	12.0	9.7	15.4
Spring	12	Ice edge	2019/10/30	2019/11/01	-59.3	-58.6	12.0	17.7	23.3	15.5
Spring	13	Ice edge	2019/11/01	2019/11/03	-58.6	-58.5	17.7	22.0	19.4	15.6
Spring	14	Ice edge	2019/11/03	2019/11/04	-58.5	-56.8	22.0	21.5	22.5	15.6
Spring	15	Ice edge	2019/11/04	2019/11/06	-56.7	-55.5	21.1	10.9	24.9	15.5
Spring	16	Ice edge/ Northbound	2019/11/06	2019/11/08	-55.5	-56.1	10.9	0.8	33.5	15.6
Spring	17	Northbound	2019/11/08	2019/11/09	-56.1	-54.0	0.5	0.0	27.5	15.6
Spring	18	Northbound	2019/11/10	2019/11/12	-51.4	-47.0	0.0	4.5	40.6	15.0
Spring	19	Northbound	2019/11/12	2019/11/13	-47.0	-43.8	4.5	7.7	21.7	14.7
Spring	20	Northbound	2019/11/13	2019/11/14	-43.7	-44.7	7.9	6.9	24.0	14.6

Spring	21	Northbound	2019/11/14	2019/11/16	-44.9	-41.5	6.7	9.6	30.0	14.6
Spring	22	Northbound	2019/11/16	2019/11/18	-41.5	-36.3	9.6	13.3	25.4	14.3
Spring	23	Northbound	2019/11/18	2019/11/19	-36.3	-36.2	13.3	13.5	7.5	14.1
Summer	1	Southbound	2018/12/07	2018/12/08	-34.5	-37.0	14.8	12.7	13.8	14.5
Summer	2	Southbound	2018/12/08	2018/12/09	-37.1	-41.8	12.6	8.8	24.8	14.9
Summer	3	Southbound	2018/12/09	2018/12/10	-41.8	-44.1	8.8	6.8	13.5	15.3
Summer	4	Southbound	2018/12/10	2018/12/12	-45.0	-50.8	6.1	0.6	14.2	16.0
Summer	5	Southbound	2018/12/14	2018/12/16	-59.7	-68.3	0.0	0.0	15.6	21.3
Summer	6	Southbound	2018/12/16	2018/12/19	-68.5	-70.1	0.0	-2.1	29.5	24
Summer	7	Southbound	2018/12/19	2018/12/21	-70.1	-70.2	-2.1	-2.1	27.1	24
Summer	8	Northbound	2019/02/27	2019/03/01	-69.3	-60.0	-4.0	-2.3	40.6	14.7
Summer	9	Northbound	2019/03/01	2019/03/03	-60.0	-59.5	-2.8	-26.1	38.8	13.9
Summer	10	Northbound	2019/03/03	2019/03/04	-59.5	-55.9	-26.1	-33.8	26.2	13.6
Summer	11	Northbound	2019/03/04	2019/03/10	-55.8	-49.5	-34.0	4.1	33.1	13.1
Summer	12	Northbound	2019/03/10	2019/03/12	-49.5	-43.1	4.1	7.8	34.1	12.7
Summer	13	Northbound	2019/03/12	2019/03/13	-43.1	-36.3	7.8	13.3	34.9	12.5
Summer	14	Northbound	2019/03/13	2019/03/14	-36.1	-34.4	13.4	17.8	18.1	12.4

Table S2. Accepted reference values for $\delta^{15}N$ vs. N_2 in air and $\delta^{18}O$ vs. VSMOW in ‰ for the calibration standards used.

Standard	**IAEA-N3**	**USGS34**	**USGS35**	**Citation**
$\delta^{15}N$	4.7	-1.8		Böhlke et al., 2003
$\delta^{18}O$	25.6	-27.9	57.5	Böhlke et al., 2003

Table S3. The pooled standard deviation in ‰ and samples size (1 SD_p; n = x) for repeated measurements of reference standards in summer and winter & spring.

Season	**Standard**	**IAEA-N3**	**USGS34**	**USGS35**
winter & spring	**$\delta^{15}N$**	0.32; n = 19	0.16; n = 19	
	$\delta^{18}O$	0.26; n = 19	0.64; n = 19	0.52, n = 19

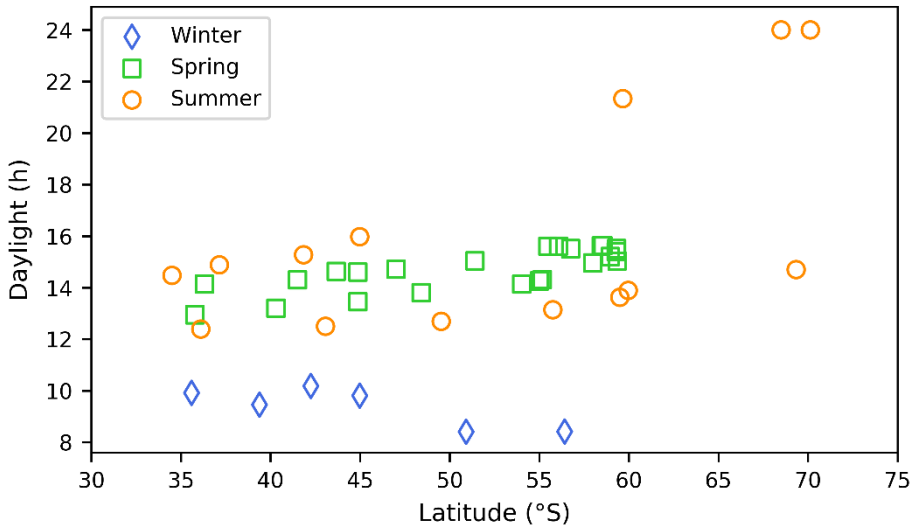

Figure S1. The number of daylight hours (h) available during each filter deployment in winter (blue diamonds), spring (green squares) and summer (orange circles), with latitude (º S).

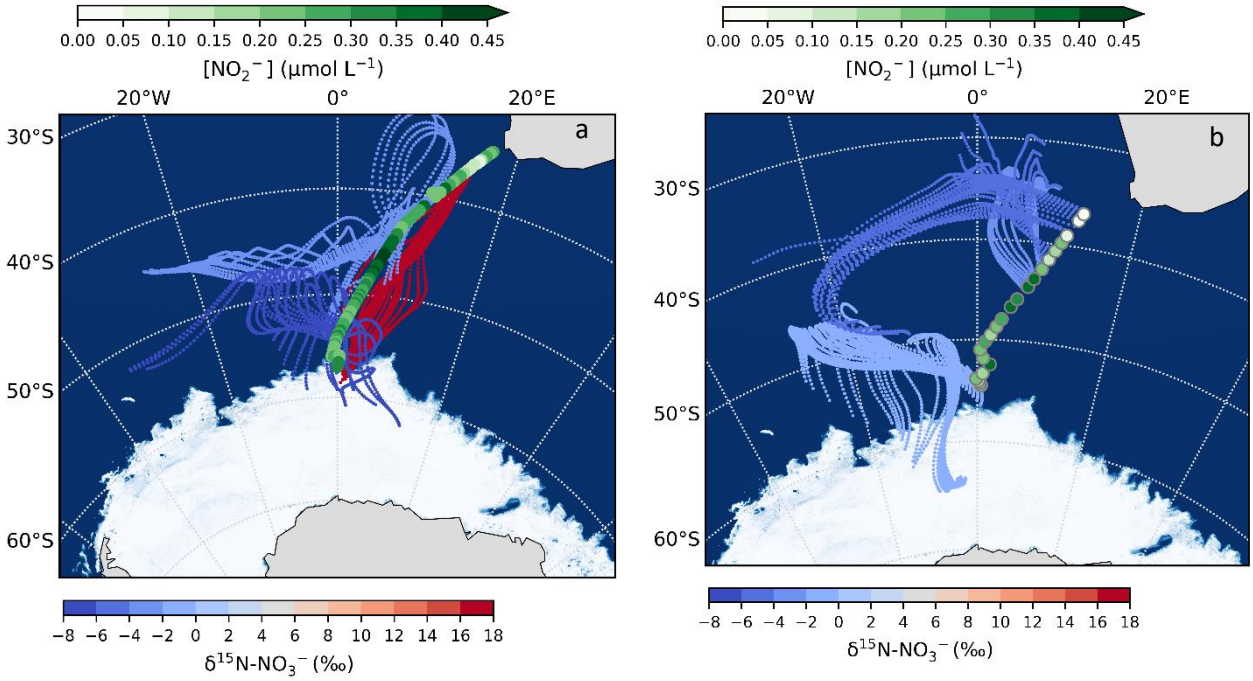

Figure S2. 72-hour AMBTs computed for each hour of the winter cruise during the southbound leg (a), the northbound leg (b) when the HV-AS was running for more than 45 min of the hour. AMBTs are colour coded by the weighted average $\delta^{15}N\text{-}NO_3^-$, represented by the blue to red colour bar. Overlaid are the surface ocean nitrite concentrations ($[NO_2^-]$), represented by the green colour bar. The white area represents the location of the sea ice determined using satellite-derived sea ice concentration data obtained from the passive microwave sensors ASMR2 (Advanced Microwave Scanning Radiometer2; Spreen et al., 2008).

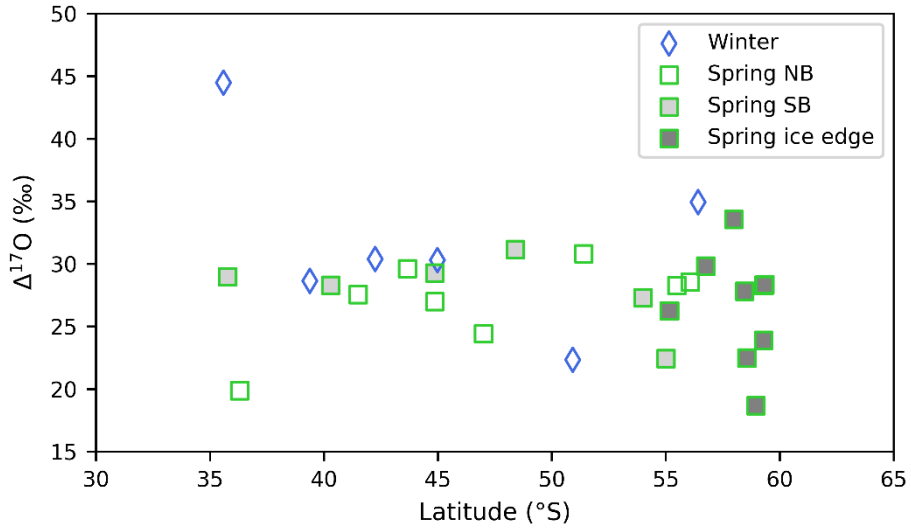

Figure S3. The weighted average $\Delta^{17}O$ of atmospheric nitrate ($\Delta^{17}O\text{-}NO_3^-$ (‰)) as a function of latitude (º S). Winter and spring are denoted by blue diamonds and green squares, respectively. Spring data are separated into northbound (NB), southbound (SB) and ice edge legs by clear, light grey and dark grey fills, respectively.

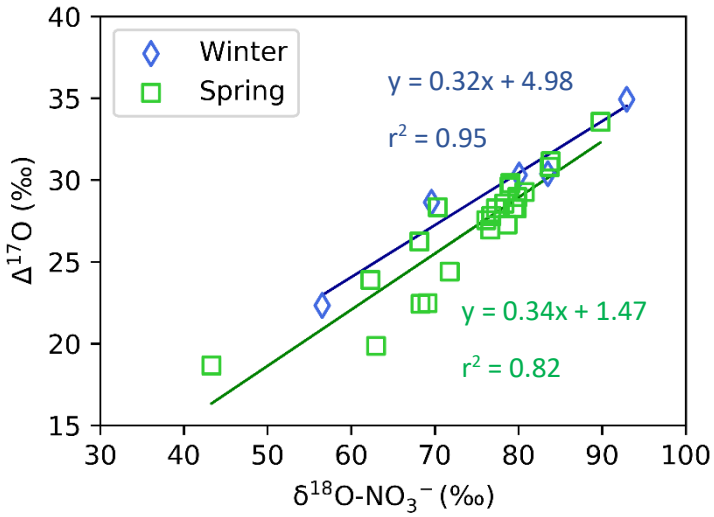

Figure S4. The correlation between atmospheric $\delta^{18}O\text{-}NO_3^-$ and $\Delta^{17}O\text{-}NO_3^-$ in winter (blue diamonds) and spring (green squares). The best fit equations and coefficients of determination (R^2) for $\delta^{18}O\text{-}NO_3^-$ vs. $\Delta^{17}O\text{-}NO_3^-$ are shown.